Acceleration of the photocatalytic degradation of organics by in-situ removal of the products of degradation

Siwada Deepracha, André Ayral, Makoto Ogawa

Acceleration of the photocatalytic degradation of organics by *in-situ* removal of the products of degradation

Siwada Deepracha[a], André Ayral[b], Makoto Ogawa[a,*]

[a]School of Energy Science and Engineering, Vidyasirimedhi Institute of Science and Technology (VISTEC), 555 Moo 1 Tumbol Payupnai, Amphoe Wangchan, Rayong 21210, Thailand

[b]Institut Européen des Membranes, IEM – UMR 5635, ENSAM, CNRS, Univ Montpellier, Montpellier, France

Corresponding Author

*E-mail: makoto.ogawa@vistec.ac.th

Abstract

Photocatalytic degradation of sulphur containing organics in water was substantially accelerated by the *in-situ* removal of sulphur oxide species formed by the dye degradation as metal sulfate precipitates. The significant enhancement of the degradation of methylene blue ($C_{16}H_{18}ClN_3S$) and acid yellow 42 ($C_{32}H_{24}N_8Na_2O_8S_2$), as examples of sulphur containing organics, was achieved when the reactions were conducted in the presence of alkaline earth cations (such as Ca^{2+}, Sr^{2+}, and Ba^{2+}).

Keywords: photocatalyst; titania; degradation; equilibrium shift

1. Introduction

Heterogeneous photocatalysis has been applied for the purification of the contaminated water by the oxidative decomposition of organic substances [1,2] and the concentration of heavy metals (As, Cd, and Cr) [3-8]. Designing structure, composition and morphology of photocatalysts has mainly been examined in order to improve the reaction efficiency [9-16].

Alternatively, improved efficiency of photocatalytic reaction has been achieved by adjusting reaction environments and conditions. The effects of pH of solution and the addition of oxidizing agent (H_2O_2) have been investigated for the decomposition of various organic dyes [17,18]. The decomposition of benzene to CO_2 was accelerated by the irradiation under magnetic field [19], and that of an azo dye (acid orange 8) was modified by the irradiation under sonication [20]. The yield and selectivity of the photocatalytic degradation of benzene was affected by the presence of photo-inactive species such as clay minerals [21]. In order to understand the mechanism of those positive effects as well as to improve the reaction efficiency further, new examples on the effects of reaction environment to affect the photocatalytic reactions are worth developing.

Here, we propose a new strategy to accelerate the decomposition of organics for wastewater treatment by chemical equilibrium shift, in which a product from the photocatalytic reaction system was removed. The idea in the present study is efficient removal of S oxide species (as sulfates) formed by the decomposition during the irradiation by capturing (*in-situ* removal) the S oxide species as precipitates of alkaline earth sulfates, which have very low solubility in water. Consequently, the dye photodegradation is expected to be promoted due to "equilibrium shift".

Sulphur containing organic compounds were selected as the target organic compounds to be decomposed. The decomposition of sulphur containing azo dyes (e.g. Procion Red, Reactive Brilliant Red, methyl orange) has been investigated in aqueous TiO_2 suspension; the N oxide species as nitrates and S oxide species as sulfates were characterized as the products in the solution after the dye decomposition [22-25]. It was reported that the amount of the sulfate formed in the solution was lower than that expected from stoichiometry [26-32], which indicated that some S oxide species were adsorbed on the surface of the photocatalyst. The adsorption of S oxide species may affect the photocatalytic reaction by blocking the catalyst's

surface for the substrate access, so that the capturing of the S oxide species from the reaction system is expected to suppress the deactivation.

2. Experimental methods

2.1. Materials

TiO_2 (Evonik P25) was purchased from Evonik Industries. Strontium nitrate anhydrous, calcium nitrate tetrahydrate, calcium acetate hydrate, methylene blue, acid yellow 42, and rhodamine 6G were purchased from Sigma-Aldrich Co., Ltd. Barium nitrate and magnesium nitrate hexahydrate were purchased from Alfa Aesar Chemical Co., Ltd. Lithium nitrate was purchased from Honeywell Fluka™. Sodium chloride and calcium chloride dihydrate was purchased from Merck Ltd. Sodium nitrate solution was prepared by equivalent molar between sodium hydroxide and nitric acid. Sodium hydroxide was purchased from Carlo Erba Reagents S.r.l. Nitric acid was purchased from Chem-Lab NV. All chemicals were used without purification.

2.2. Preparation of photocatalyst film

The photocatalyst film was prepared by casting an aqueous TiO_2 (P25) suspension onto borosilicate glass slides. The suspension was prepared by adding 0.1 g of P25 into 100 ml of DI water with magnetic stirring. Then, 0.8 ml of the P25 suspension was dropped on one side of the borosilicate glass slide and dried at room temperature. The suspension was naturally spread on the glass slide thanks to the wettability of the glass slide after the cleaning with 0.001 M of aqueous HCl solution for 1 day. The weight of P25 on the glass slide (ca. around 0.0008 g) was confirmed by measuring the weight increase after casting and drying.

2.3. Photocatalytic decomposition experiments

The photocatalytic decomposition of the S containing organic dyes (methylene blue and acid yellow 42) and the organic dye without S (rhodamine 6G) was carried out by putting the

film in an aqueous solution of the dyes and irradiated by a UV light (Eurosolar type 795 S Solaria Facial Tanning Sun Face Tanner UV Type 3 as a light source) using four UV lamps Philips CLEO 15 W. The film was immerged into the solution before UV irradiated for 1 h to examine the adsorption of dyes on the TiO_2 surface. To evaluate the role of alkaline earth cations (Ca^{2+}, Sr^{2+}, and Ba^{2+}) on the decomposition of the dyes, the anhydrous strontium nitrate, calcium nitrate tetrahydrate or barium nitrate was added into the dye solutions (initial concentration of the dye at 30 mg/L) as the source of Ca^{2+}, Sr^{2+}, and Ba^{2+} with fixing concentration of alkaline earth cations at 0.5 M, respectively. The photocatalytic decomposition of the dyes in the presence of sodium chloride, sodium nitrate, and lithium nitrate (as the source of Na^{+} and Li^{+}) was further examined to confirm the proposed mechanism under the identical conditions (0.5 M of concentration of the inorganic salts). The effects of co-existing anions on the decomposition of the dyes was examined by adding the 0.5 M of calcium chloride into the solution. The pH of the solution before and after adding alkaline earth cations was measured by pH meter (HANNA, HI2004 edge). The irradiance was 0.01 W/cm^2, measured at distance between the light source and the photocatalyst film by EIT Power UV Radiometer, 92380 GARCHES S/N0491029. The concentration of the dyes after the reaction was directly determined by using JENWAY 7315 Spectrophotometer without any separation processes of powder thanks to advantages of film application and the changes of the concentration of the dyes (the absorbance at 664 nm for methylene blue, at 440 nm for acid yellow 42, and at 530 nm for rhodamine 6G) during irradiation were followed.

2.4. Kinetic analyses

Apparent pseudo first-order decomposition rate constant (k) was determined for the evaluation the photocatalytic decomposition of the dyes in the presence and the absence of alkaline earth cations in the solution. The rate constant (k = slope) is derived by the graph

relationship between $\ln(C_0/C_t)$ versus irradiation time, where C_0 is initial concentration of the dyes and C_t is concentration of the dyes after the reaction at time t.

3. Results and discussion

3.1. Morphology and the advantages of the photocatalyst film

In the preliminary experiments using the titania photocatalyst (P25, Evonik, average particle size of 22 nm from Aerosil Co., Ltd.) suspension, the state of the suspension was significantly affected by the presence of metal salts (cause agglomeration and sedimentation, as shown in Fig. S1). In order to avoid the effects of the difference (light scattering, diffusion of reactant etc.) on the photocatalytic reaction, a film of photocatalyst was used in the present study. P25 was employed as the photocatalyst due to its high efficiency for the photocatalytic decomposition of organics and the stability of aqueous suspension. The aqueous suspension was used to prepare homogeneous film on substrate by simple casting [33,34]. The photograph of the P25 film and the SEM images are shown in Fig. 1. The film thickness was around 1.0 μm with the estimated porosity of 67% based on the calculation from the volume of solid content (0.0008 g of P25 on the substrate and the density of P25, 3.9 g/cm^3) and the estimated total volume of the film (6.25 cm^2 of the coating area and 1.0 μm of the film thickness). The porosity of random close packing of dense spherical particles is ~36% with the assumption for monodispersed particles [35]. The higher porosity of the film (67%) was explained by the sparse aggregation of P25 particles during drying, leading to interconnected pore between the P25 particles as seen in the surface morphology of the film (Fig. 1c). Thanks to the thickness (1.0 μm) and the high porosity (67%) of the film, the diffusion of organic molecules inside the particle voids is expected to be easy and all P25 particles in the layer film are photocatalytically active [36]. As the TiO_2 was immobilized on the substrate, alkaline earth sulfate formed after the reaction was expected to be observed by naked eyes as precipitates. Moreover, it was

possible to determine the change of the concentration of the organics without the separation of photocatalyst from the reaction mixture.

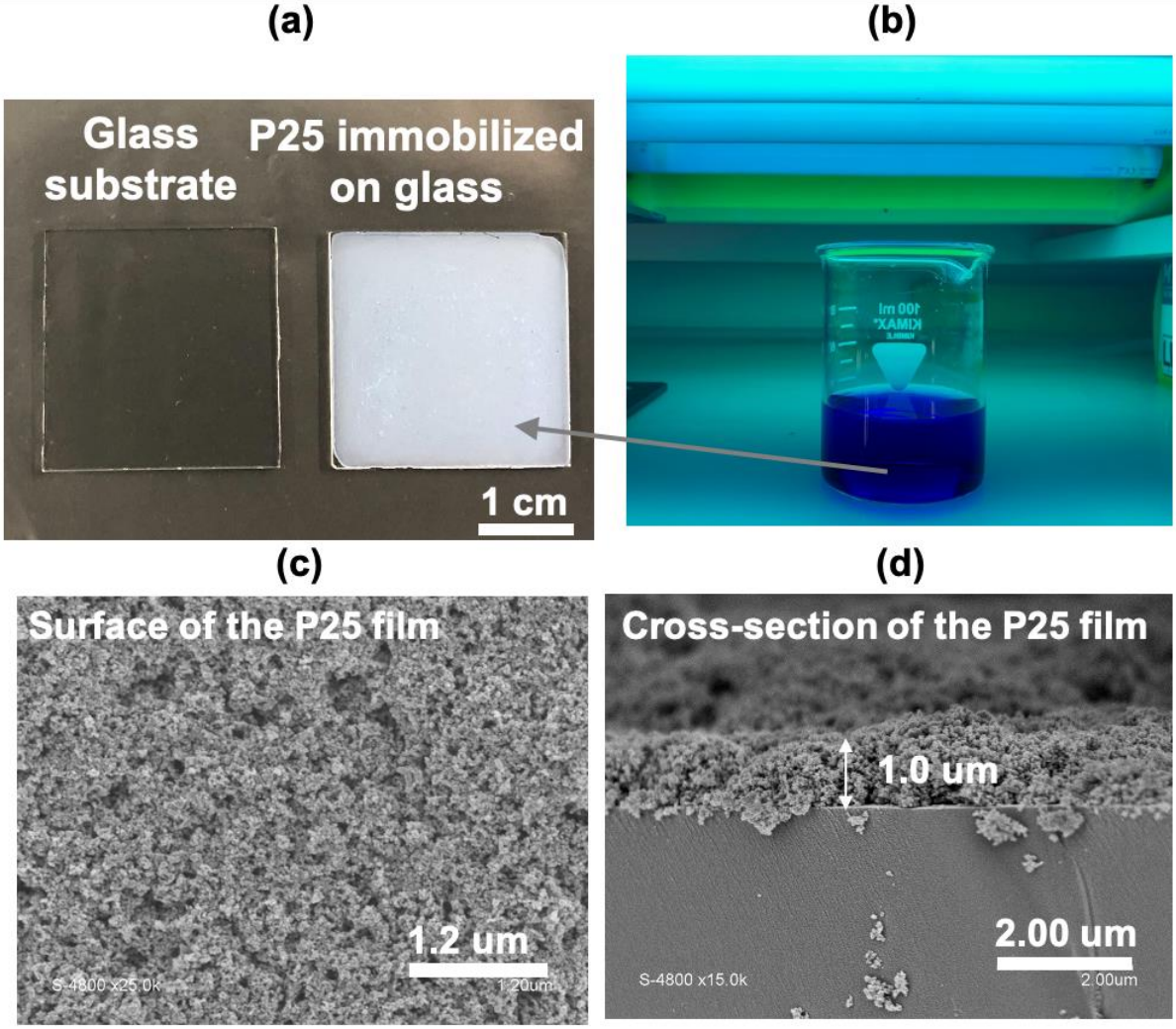

Fig. 1. (a) Photograph of the P25 immobilized on glass as the film. (b) Experimental set-up by putting the P25 film into the solutions. (c) Surface and (d) cross-section images of the P25 film from SEM observations.

3.2. Photocatalytic decomposition of sulphur-containing organics

Methylene blue ($C_{16}H_{18}ClN_3S$, abbreviated as MB) was selected as a sulphur containing organic. The photocatalytic decomposition of MB was carried out in the absence or presence of an alkaline cation, Na^+ (adding NaCl), or of alkaline earth cations such as Ca^{2+}, Sr^{2+}, and

Ba^{2+} (adding $Ca(NO_3)_2$, $Sr(NO_3)_2$, and $Ba(NO_3)_2$) in the solution, respectively (Fig. 2a). The decomposition of MB was accelerated when the reaction was conducted in the presence of Ca^{2+}, Sr^{2+}, and Ba^{2+} (Fig. 2b). When the reaction was conducted in the presence of Na^+ in the solution, the decomposition rate was not improved and slightly retarded after the UV irradiation for 2 h. The adsorption of MB on the P25 film has here to be discussed considering the surface charge of titania. The pH of solution changed from 6.48 to 6.41, 5.86, 5.91, and 5.64 after the addition of NaCl, $Ca(NO_3)_2$, $Sr(NO_3)_2$, $Ba(NO_3)_2$ in the solution, respectively. The isoelectric point of P25 is reported to be around 6 [37]. Adsorption of MB on the P25 film was not observed for the reaction in $Ca(NO_3)_2$, $Sr(NO_3)_2$, and $Ba(NO_3)_2$ solutions. The adsorption of humic acid on TiO_2 was before claimed as the main reason to promote the decomposition of humic acid in aqueous suspension containing Ca^{2+} [38]. The present phenomena are therefore not explained by the effects of the MB adsorption.

The decomposition of MB in the presence of $Mg(NO_3)_2$, $LiNO_3$ and $NaNO_3$ was also examined. The concentration of MB decreased from 30 ppm to 27 ppm by the addition of $Mg(NO_3)_2$, $LiNO_3$, and $NaNO_3$ into the MB solution in the dark, suggesting that the adsorption of MB on P25 by the electrostatic interactions happened to some extent by the change of pH (from 6.48 to 7.32, 9.21, and 12.10 for $Mg(NO_3)_2$, $LiNO_3$ and $NaNO_3$ systems, respectively).

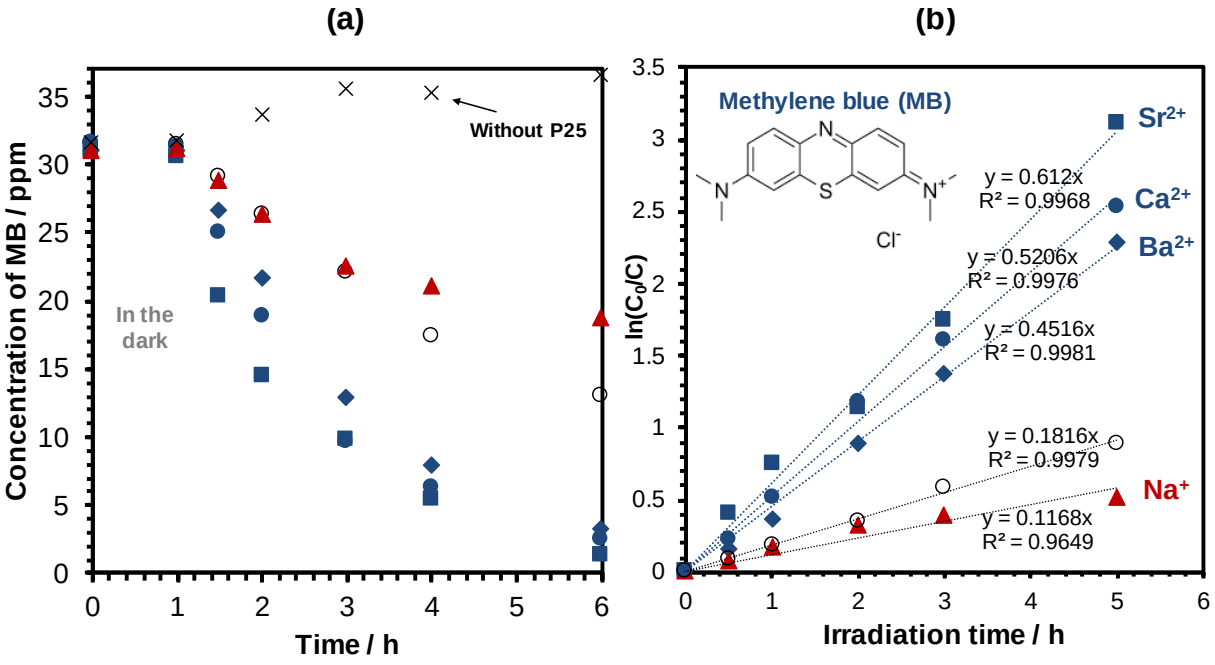

Fig. 2. Photocatalytic decomposition of (a) MB and (b) apparent pseudo first order plot of the MB decomposition by using the P25 film in the absence (black open circle) and the presence of Na^+ (red triangle) and alkaline earth cations (Ca^{2+}; blue full circle, Sr^{2+}; blue square, and Ba^{2+}; blue diamond) by adding NaCl, $Ca(NO_3)_2$, $Sr(NO_3)_2$, and $Ba(NO_3)_2$ in the solution, respectively.

An anionic dye, acid yellow 42 ($C_{32}H_{24}N_8Na_2O_8S_2$, abbreviated as AY42), was chosen as another example of sulphur containing organics to be examined for the photocatalytic decomposition in the presence of metal salts. The photocatalytic decomposition of AY42 was successfully accelerated in the presence of Ca^{2+}, Sr^{2+} and Ba^{2+}, whereas no significant effects on the decomposition of AY42 were observed by the addition of Mg^{2+}, Na^+ and Li^+ (Fig. 3a). The decomposition of AY42 was also accelerated when $CaCl_2$ was added. Thus, the decomposition rate of MB and AY42 was accelerated by the presence of Ca^{2+}, Sr^{2+} and Ba^{2+}, and was not affected by the co-existing anions (NO_3^- or Cl^-). The rate constants of the decomposition of AY42 were 0.83, 1.17, and 1.14 h^{-1} for the reactions in the presence of Ba^{2+}, Ca^{2+}, and Sr^{2+}, respectively (Fig. 3b). The decomposition of AY42 was faster than that of MB

under the present conditions, which is thought to be due to the difference in the decomposition pathways of AY42 and MB [31].

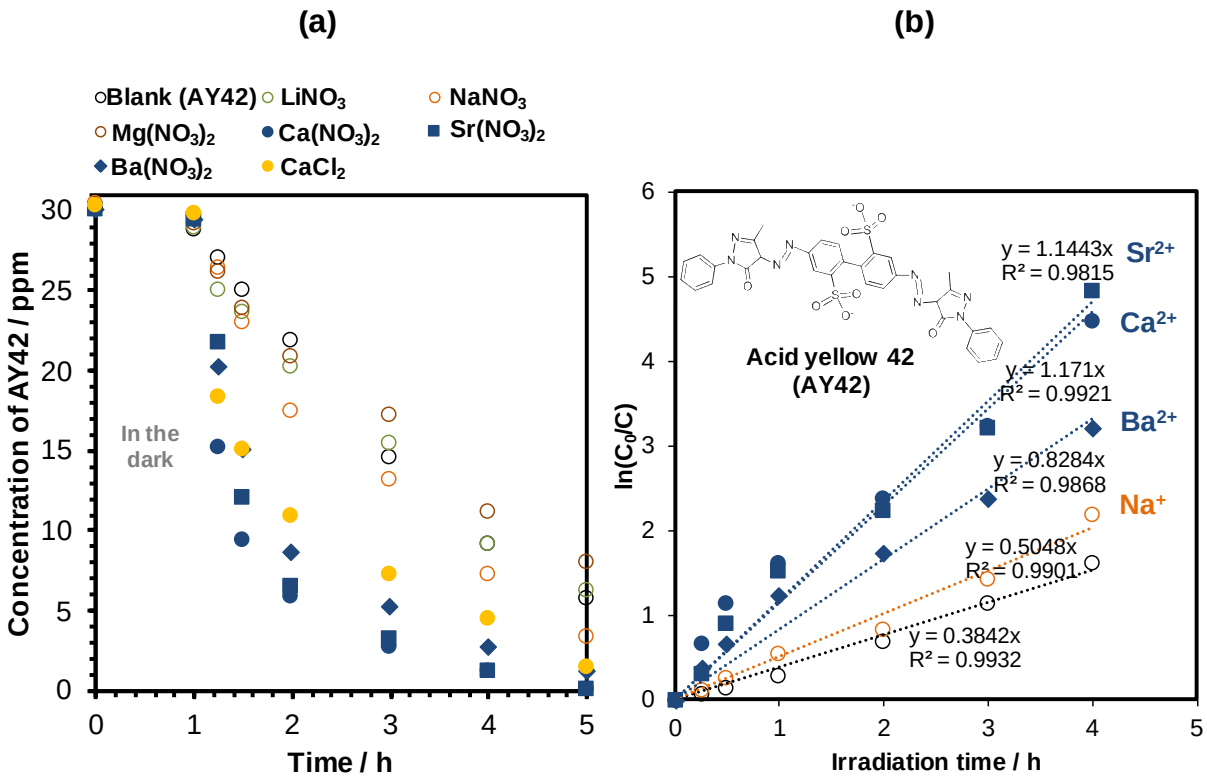

Fig. 3. (a) Photocatalytic decomposition of AY42 and (b) apparent pseudo first order plot of the AY42 decomposition by using the P25 film in the absence and the presence of inorganic salts such as $LiNO_3$, $NaNO_3$, $Mg(NO_3)_2$, $Ca(NO_3)_2$, $CaCl_2$, $Sr(NO_3)_2$, and $Ba(NO_3)_2$.

3.3. Photocatalytic decomposition of organic without sulphur in the chemical structure

The decomposition of Rhodamine 6G ($C_{28}H_{31}ClN_2O_3$, abbreviated as R6G), which is a dye without sulphur in its structure, was examined in the presence of Ca^{2+} (by adding $CaCl_2$ or $Ca(COOCH_3)_2$ into the solution). It was reported that nitrate ions can interact with R6G to show the decrease of the concentration [39], so that calcium nitrate was not used to examine the decomposition of R6G in the present study. The changes in the concentration by the UV irradiation are shown in Fig. 4. The decomposition of R6G was not accelerated by the presence

of Ca^{2+}, supporting the important role of the *in-situ* removal of the sulphur containing species on the photodegradation of sulphur containing organics.

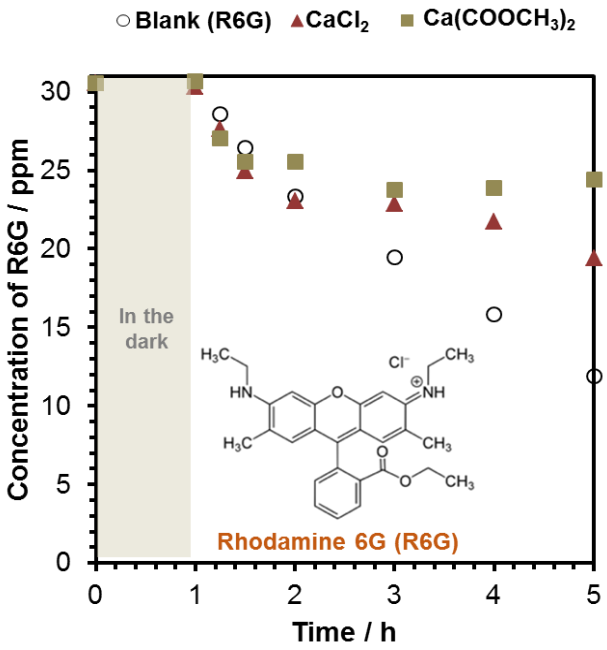

Fig. 4. Photocatalytic decomposition of R6G in the absence and the presence of Ca^{2+} by adding $CaCl_2$ or $Ca(COOCH_3)_2$ in the solution.

3.4. Proposed mechanism for the accelerated photodegradation of sulphur containing organics

Precipitate was clearly observed as the sediment after the decomposition of MB in the presence of Ca^{2+} (Fig. 5a), while the amount of the precipitate was too small to be collected for its identification. The amount of $CaSO_4$ which may be formed considering the sulfate anions resulting from MB oxidation, is estimated to 0.13 mg based on the stoichiometric calculation assuming the complete decomposition of the MB in the starting solution. The presence of sulfate ions formed in the solution after the decomposition of MB in the presence of Ca^{2+} and Na^{+} for 16 h (colorless solutions) was examined by ion chromatography, as shown in Fig. 5b. The concentration of sulfate ions in the solution containing Ca^{2+} and Na^{+} were 0.4 and to 6.4 $mg.L^{-1}$, respectively. Assuming the complete decomposition of MB, the estimated

concentration of sulfate ions in the solution is 9 $mg.L^{-1}$. It was thought that the sulfate ions were removed from the solution by the precipitation with Ca^{2+} as $CaSO_4$.

The concentration of sulfate ions required for the formation of alkaline earth sulfates is calculated to be 4.6, 0.05, and 2.1×10^{-5} $mg.L^{-1}$ for $CaSO_4$, $SrSO_4$ and $BaSO_4$, respectively, from solubility equilibrium's equation using the initial concentration of alkaline earth cations (0.5 $mol.L^{-1}$) and the solubility product constant (K_{sp}) of 2.4×10^{-5}, 2.51×10^{-6}, and 1.07×10^{-10} for $CaSO_4$, $SrSO_4$ and $BaSO_4$ [40,41], respectively. Those values were lower than the expected concentration of sulfate ions in the present experiment after the complete decomposition of MB (ca. 9 $mg.L^{-1}$), meaning that the precipitation of $CaSO_4$, $SrSO_4$ and $BaSO_4$ was possible from the concentration of the sulfate ions formed by the decomposition of MB.

The observed effect of the additives on the improved efficiency of the degradation of sulphur containing organics (AY42 and MB) is proposed to be a "chemical equilibrium shift", where the product (sulfate) was removed during the reactions by the alkaline earth cations (Ca^{2+}, Ba^{2+}, and Sr^{2+}) as sulfate precipitation. The presence of the precipitates and the loss of sulfate ions in the solution during the irradiation are the evidences of the removal of S oxide species as metal (Ca^{2+}, Ba^{2+}, and Sr^{2+}) sulfates.

In addition to the equilibrium shift concept, the deactivation of TiO_2 by the adsorption of S oxide species was suppressed as another positive aspect of the present strategy. The film was re-used to obtain the similar results for the MB decomposition in the absence and the presence of Ca^{2+} (Fig. S2). The efficient MB decomposition was found in the second and third runs in the presence of Ca^{2+}, while the decomposition of MB was retarded when the P25 film was re-used for the reaction in the absence of Ca^{2+}. These were consistent with the relatively white color of the P25 film after the reactions in the presence of Ca^{2+}, Sr^{2+}, and Ba^{2+}, when compared with the P25 film after the reactions without adding such ions as Ca^{2+}, Ba^{2+}, and Sr^{2+}, or in the presence of Na^{+} (Fig. 5c). Therefore, the simultaneous prevention of S oxide

species adsorption on the catalysts and the efficient removal of product (as sulfates) are clarified as two possible mechanisms on the acceleration of MB decomposition.

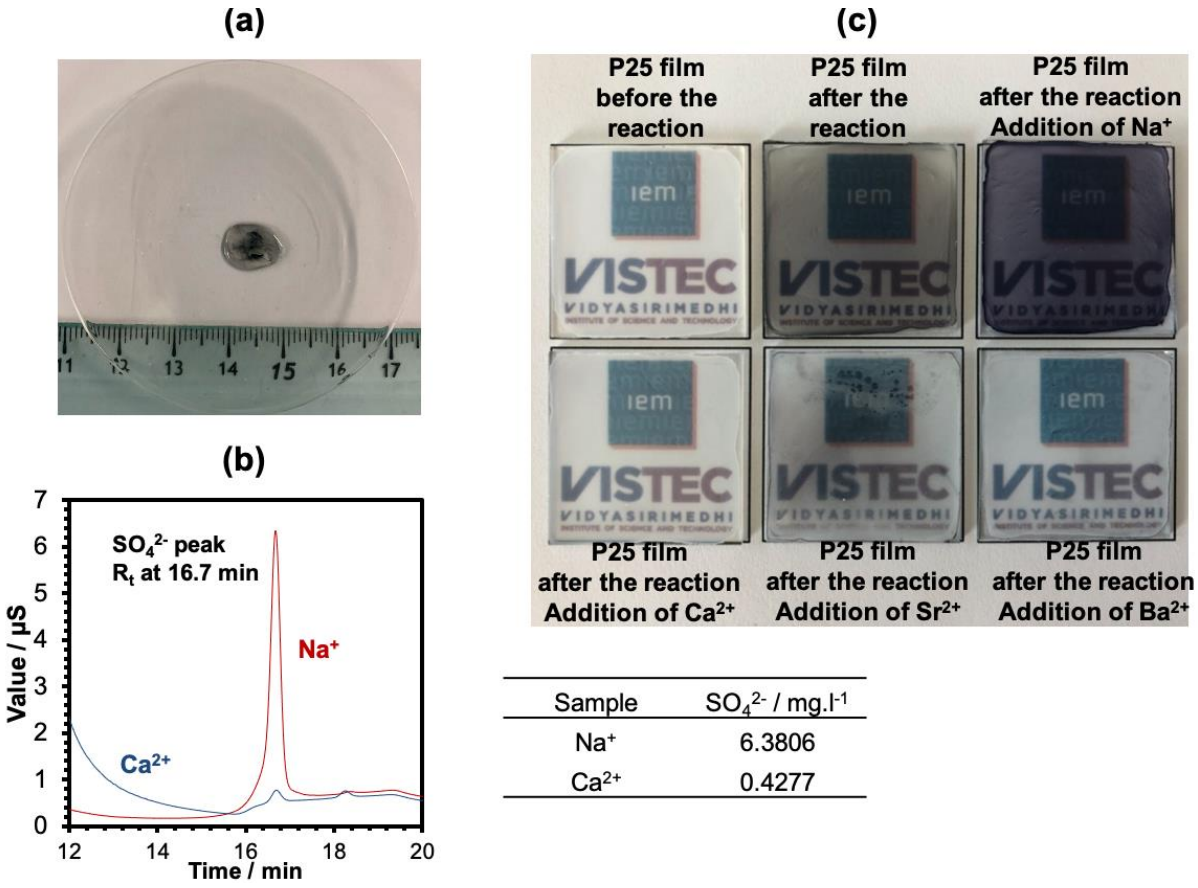

Sample	SO_4^{2-} / mg.l^{-1}
Na^+	6.3806
Ca^{2+}	0.4277

Fig. 5. (a) Photograph of precipitated powder after the decomposition of MB in the presence of Ca^{2+}. (b) Characterization of sulfate ions remaining in the solution by Ion Chromatography. (c) Photographs of the P25 film before and after the reaction.

The effects of the added inorganic cations (such as K^+, Na^+, Ca^{2+} and Mg^{2+}) [42-49] and anions (such as Cl^-, SO_4^{2-} and NO_3^-) [50-57] on the decomposition of various organics have been reported in the literature, where the reactions were conducted in aqueous TiO_2 suspensions. For the reactions in the presence of Ca^{2+}, no significant acceleration was found on the decomposition of phenol [42,43], crystal violet [44], and glyphosate [45], while negative effects were observed for the decomposition of rhodamine B [46], nicosulfuron [47], and formic acid [48]. The adsorption of the added inorganic cation (Ca^{2+}) and anions (SO_4^{2-}) onto

the photocatalyst (TiO_2) was claimed as a reason of the inhibition of the decomposition of nicosulfuron by blocking the accessible surface of TiO_2. The sedimentation of P25 was observed in the aqueous suspension by the addition of Ca^{2+} salts (Fig. S1). The sedimentation of P25 in the aqueous suspension is thought to affect the decomposition rate of MB by losing the active surface for the reaction by the aggregation of P25 and also by increasing the diffusion path from the solution to the active surface in the core of the formed aggregates as well as the loss of incident light propagation. Thus, the decomposition efficiency in the aqueous suspension of TiO_2 is difficult to be directly compared with the result achieved in the present study by using P25 film as the photocatalysts. The application of P25 film in this work is a key from the viewpoint of the product characterization.

4. Conclusions

The decomposition of the sulphur containing organics (MB and AY42) was successfully accelerated for the first time by adding inorganic cations (alkaline earth cations) to capture the S oxide species (as sulfates) formed during the decomposition. Since the commonly used suspension of photocatalysts cause the aggregation during the reaction, the film of P25 supported on borosilicate glass was used as the photocatalyst, which was a key of the present success. The acceleration was explained by the two mechanisms, equilibrium shift and the suppressed poisoning (deactivation) of the catalyst's surface with sulfate. The present concept (*in-situ* removal of a product) can be applied various photocatalytic reactions to be accelerated.

CRediT authorship contribution statement

Siwada Deepracha: Methodology, Formal analysis, Investigation, Writing – Original Draft, Writing – Review & Editing. **André Ayral:** Validation, Formal analysis, Resources,

Writing – Review & Editing. **Makoto Ogawa:** Conceptualization, Validation, Writing – Review & Editing, Supervision.

Declaration of Competing Interest

The authors declare that they have no known competing financial interests or personal relationships that could have appeared to influence the work reported in this paper.

Acknowlegments

This work was supported by the Research Chair Grant 2017 (grant number FDA-CO-2560-5655) from the National Science and Technology Development Agency (NSTDA), Thailand. One of the authors (S. Deepracha) acknowledges Vidyasirimedhi Institute of Science and Technology for the scholarship to his Ph.D. study. The authors would like to thank Ms. Valérie Bonniol for the help on ion chromatography analyses and Mr. Didier Cot for the help on SEM observation.

Appendix A. Supplementary data

Photocatalytic decomposition of MB by the P25 dispersed in the aqueous MB solution with and without addition of $Ca(NO_3)_2$, photograph of the P25 dispersed in water with and without addition of $Ca(NO_3)_2$, and reuse of the photocatalyst film for the photocatalytic decomposition of MB

References

[1] L. Max, P. Pichat, Photocatalysis and water purification; from fundamentals to recent applications, Wiley-VCH, Germany, 2013.

[2] K. Kabra, R. Chaudhary, R.L. Sawhney, Treatment of hazardous organic and inorganic compounds through aqueous-phase photocatalysis: a review, Ind. Eng. Chem. Res. 43 (2004) 7683-7696.

[3] X. Guan, J. Du, X. Meng, Y. Sun, B. Sun, Q. Hu, Application of titanium dioxide in arsenic removal from water: a review, J. Hazard. Mater. 215 (2012) 1-16.

[4] X. Bai, Y. Du, X. Hu, Y. He, C. He, E. Liu, J. Fan, Synergy removal of Cr (VI) and organic pollutants over RP-MoS_2/rGO photocatalyst, Appl. Catal. B 239 (2018) 204-213.

[5] S. Ghosh, H. Remita, R.N. Basu, Visible-light-induced reduction of Cr (VI) by PDPB-ZnO nanohybrids and its photo-electrochemical response, Appl. Catal. B 239 (2018) 362-372.

[6] R. Vinu, G. Madras, Kinetics of simultaneous photocatalytic degradation of phenolic compounds and reduction of metal ions with nano-TiO_2, Environ. Sci. Technol. 42 (2012) 913-919.

[7] X.J. Zhang, T.Y. Ma, Z.Y. Yuan, Titania-phosphonate hybrid porous materials: preparation, photocatalytic activity and heavy metal ion adsorption, J. Mater. Chem. 18 (2008) 2003-2010.

[8] S. Huang, L. Gu, N. Zhu, K. Feng, H. Yuan, Z. Lou, Y. Li, A. Shan, Heavy metal recovery from electroplating wastewater by synthesis of mixed-Fe_3O_4@SiO_2/metal oxide magnetite photocatalysts, Green Chem. 16 (2008) 2696-2705.

[9] H. Yamashita, K. Mori, Y. Kuwahara, T. Kamegawa, M. Wen, P. Verma, M. Che, Single-site and nano-confined photocatalysts designed in porous materials for environmental uses and solar fuels, Chem. Soc. Rev. 47 (2018) 8072-8096.

[10] A. Kudo, Y. Miseki, Heterogeneous photocatalyst materials for water splitting, Chem. Soc. Rev. 38 (2009) 253-278.

[11] K. Maeda, K. Domen, Solid solution of GaN and ZnO as a stable photocatalyst for overall water splitting under visible light, Chem. Mater. 22 (2010) 612-623.

[12] T.W. Kim, S.J. Hwang, S.H. Jhung, J.S. Chang, H. Park, W. Choi, J.H. Choy, Bifunctional heterogeneous catalysts for selective epoxidation and visible light driven photolysis: nickel oxide-containing porous nanocomposite, Adv. Mater. 20 (2008) 539-542.

[13] X. Huang, Y. Chen, E. Walter, M. Zong, Y. Wang, X. Zhang, O. Qafoku, Z. Wang, K.M. Rosso, Facet-specific photocatalytic degradation of organics by heterogeneous fenton chemistry on hematite nanoparticles, Environ. Sci. Technol. 53 (2019) 10197-10207.

[14] D. Zhang, C. Lee, H. Javed, P. Yu, J.H. Kim, P.J. Alvarez, Easily recoverable, micrometer-sized TiO_2 hierarchical spheres decorated with cyclodextrin for enhanced photocatalytic degradation of organic micropollutants, Environ. Sci. Technol. 52 (2018) 12402-12411.

[15] L. Guo, Y. Jing, B.P. Chaplin, Development and characterization of ultrafiltration TiO_2 magnéli phase reactive electrochemical membranes, Environ. Sci. Technol. 50 (2016) 1428-1436.

[16] Z. Xiong, J. Ma, W.J. Ng, T.D. Waite, X.S. Zhao, Silver-modified mesoporous TiO_2 photocatalyst for water purification, Water Res. 45 (2011) 2095-2103.

[17] I.K. Konstantinou, T.A. Albanis, TiO_2-assisted photocatalytic degradation of azo dyes in aqueous solution: kinetic and mechanistic investigations: a review, Appl. Catal. B 49 (2004) 1-14.

[18] Y. Ye, Y. Feng, H. Bruning, D. Yntema, H.H.M. Rijnaarts, Photocatalytic degradation of metoprolol by TiO_2 nanotube arrays and UV-LED: Effects of catalyst properties, operational parameters, commonly present water constituents, and photo-induced reactive species, Appl. Catal. B 220 (2018) 171-181.

[19] W. Zhang, X. Wang, X. Fu, Magnetic field effect on photocatalytic degradation of benzene over Pt/TiO_2, Chem. Commun. (2003) 2196-2197.

[20] E. Selli, Synergistic effects of sonolysis combined with photocatalysis in the degradation of an azo dye, Phys. Chem. Chem. Phys. 4 (2002) 6123-6128.

[21] Y. Ide, M. Matsuoka, M. Ogawa, Controlled photocatalytic oxidation of benzene in aqueous clay suspension, ChemCatChem 4 (2012) 628-630.

[22] F. Lin, Y. Zhang, L. Wang, Y. Zhang, D. Wang, M. Yang, J. Yang, B. Zhang, Z. Jiang, C. Li, Highly efficient photocatalytic oxidation of sulfur-containing organic compounds and dyes on TiO_2 with dual cocatalysts Pt and RuO_2, Appl. Catal. B 127 (2012) 363-370.

[23] C. Hu, C.Y. Jimmy, Z. Hao, P.K. Wong, Photocatalytic degradation of triazine-containing azo dyes in aqueous TiO_2 suspensions, Appl. Catal. B 42 (2003) 47-55.

[24] V. Augugliaro, C. Baiocchi, A.B. Prevot, E. García-López, V. Loddo, S. Malato, G. Marcí, L. Palmisano, M. Pazzi, E. Pramauro, Azo-dyes photocatalytic degradation in aqueous suspension of TiO_2 under solar irradiation, Chemosphere 49 (2002) 1223-1230.

[25] M. Vautier, C. Guillard, J.M. Herrmann, Photocatalytic degradation of dyes in water: case study of indigo and of indigo carmine, J. Catal. 201 (2001) 46-59.

[26] F. He, U. Muliane, S. Weon, W. Choi, Substrate-specific mineralization and deactivation behaviors of TiO_2 as an air-cleaning photocatalyst, Appl. Catal. B (2020) 119145.

[27] N.M. Mahmoodi, M. Arami, N.Y. Limaee, K. Gharanjig, F.D. Ardejani, Decolorization and mineralization of textile dyes at solution bulk by heterogenous nanophotocatalysis using immobilized nanoparticles of titanium dioxide, Colloids Surf. A 290 (2006) 125-131.

[28] N. González-García, J.A. Ayllón, X. Doménech, J. Peral, TiO_2 deactivation during the gas-phase photocatalytic oxidation of dimethyl sulfide, Appl. Catal. B 52 (2004) 69-77.

[29] C.H. Ao, S.C. Lee, S.C. Zou, C.L. Mak, Inhibition effect of SO_2 on NO_x and VOCs during the photodegradation of synchronous indoor air pollutants at parts per billion (ppb) level by TiO_2, Appl. Catal. B 49 (2004) 187-193.

[30] M. Karkmaz, E. Puzenat, C. Guillard, J.M. Herrmann, Photocatalytic degradation of the alimentary azo dye amaranth: Mineralization of the azo group to nitrogen, Appl. Catal. B 51 (2004) 183-194.

[31] H. Lachheb, E. Puzenat, A. Houas, M. Ksibi, E. Elaloui, C. Guillard, J.M. Herrmann, Photocatalytic degradation of various types of dyes (alizarin S, crocein orange G, methyl red, congo red, methylene blue) in water by UV-irradiated titania, Appl. Catal. B 39 (2002) 75-90.

[32] M. Stylidi, D.I. Kondarides, X.E. Verykios, Pathways of solar light-induced photocatalytic degradation of azo dyes in aqueous TiO_2 suspension, Appl. Catal. B 40 (2003) 271-286.

[33] S. Deepracha, S. Bureekaew, M. Ogawa, Synergy effects of the complexation of a titania and a smectite on the film formation and its photocatalyst' performance, Appl. Clay Sci. 169 (2019) 129-134.

[34] T. Goto, M. Ogawa, Visible light responsive photocatalytic flow reactor composed of titania film photosensitized by metal complex-clay hybrid, ACS Appl. Mater. Interfaces 7 (2015) 12631-12634.

[35] F.A. Dullien, Porous media: fluid transport and pore structure, Academic press, Elsevier, United States, 2012.

[36] D. Chen, F. Li, A.K. Ray, Effect of mass transfer and catalyst layer thickness on photocatalytic reaction, AIChE J. 46 (2000) 1034-1045.

[37] M. Kosmulski, Isoelectric points and points of zero charge of metal (hydr) oxides: 50 years after Parks' review, Adv. Colloid Interface Sci. 238 (2016) 1-61.

[38] X.Z. Li, C.M. Fan, Y.P. Sun, Enhancement of photocatalytic oxidation of humic acid in TiO_2 suspensions by increasing cations strength, Chemosphere 48 (2002) 453-460.

[39] L. Wang, B. Li, L. Zhang, L. Zhang, H. Zhao, Fabrication and characterization of a fluorescent sensor based on Rh6G-functionalized silica nanoparticles for nitrite ion detection, Sensor Actuat. B-Chem. 171 (2002) 946-953.

[40] W.I. Stephen, A. Ringbom, Complexation in analytical chemistry: Interscience Publishers, John Wiley & Sons, New York, 1965.

[41] B.S. Krumgalz, Temperature dependence of mineral solubility in water. Part 3. Alkaline and alkaline earth sulfates, J. Phys. Chem. Ref. Data 47 (2018) 023101.

[42] N. Kashif, F. Ouyang, Parameter effect on heterogeneous photocatalyzed degradation of phenol in aqueous dispersion of TiO_2, Environ. Sci. Technol. 21 (2009) 527-533.

[43] V. Brezová, A. Blažková, E. Borošová, M. Čeppan, R. Fiala, The influence of dissolved metal ions on the photocatalytic degradation of phenol in aqueous TiO_2 suspension, J. Mol. Catal. A-Chem 98 (1995) 109-116.

[44] C. Sahoo, A. Gupta, A. Pal, Photocatalytic degradation of crystal violet (CI Basic Violet 3) on silver ion doped TiO_2, Dyes Pigm. 66 (2005) 189-196.

[45] S. Chen, Y. Liu, Study on the photocatalytic degradation of glyphosate by TiO_2 photocatalyst, Chemosphere 67 (2007) 1010-1017.

[46] M. Makita, A. Harata, Photocatalytic decolorization of rhodamine B dye as a model of dissolved organic compounds: Influence of dissolved inorganic chloride salts in seawater of the Sea of Japan, Chem. Eng. Process 47 (2008) 859-863.

[47] A.M. Dugandžić, A.V. Tomašević, M.M. Radišić, N.Ž. Šekuljica, D.Ž. Mijin, S.D. Petrović, Effect of inorganic ions, photosensitizers and scavengers on the photocatalytic degradation of nicosulfuron, J. Photochem. Photobiol. A 336 (2017) 146-155.

[48] N. Negishi, Y. Miyazaki, S. Kato, Y. Yang, Effect of HCO_3^- concentration in groundwater on TiO_2 photocatalytic water purification, Appl. Catal. B 242 (2019) 449-459.

[49] S. Sontakke, J. Modak, G. Madras, Effect of inorganic ions, H_2O_2 and pH on the photocatalytic inactivation of Escherichia coli with silver impregnated combustion synthesized TiO_2 catalyst, Appl. Catal. B 106 (2011) 453-459.

[50] J.C. Crittenden, Y. Zhang, D.W. Hand, D.L. Perram, E.G. Marchand, Solar detoxification of fuel-contaminated groundwater using fixed-bed photocatalysts, Water Environ. Res. 68 (1996) 270-278.

399 [51] D.C. Schmelling, K.A. Gray, P.V. Kamat, The influence of solution matrix on the
400 photocatalytic degradation of TNT in TiO_2 slurries, Water Res. 31 (1997) 1439-1447.
401 [52] M.H. Habibi, A. Hassanzadeh, S. Mahdavi, The effect of operational parameters on the
402 photocatalytic degradation of three textile azo dyes in aqueous TiO_2 suspension, J. Photochem.
403 Photobiol. A 172 (2005) 89-96.
404 [53] A.G. Rincon, C. Pulgarin, Effect of pH, inorganic ions, organic matter and H_2O_2 on E.
405 coli K12 photocatalytic inactivation by TiO_2: implications in solar water disinfection, Appl.
406 Catal. B 51 (2004) 283-302.
407 [54] C. Guillard, H. Lachheb, A. Houas, M. Ksibi, E. Elaloui, J.M. Herrmann, Influence of
408 chemical structure of dyes, of pH and of inorganic salts on their photocatalytic degradation by
409 TiO_2 comparison of the efficiency of powder and supported TiO_2, J. Photochem. Photobiol. A
410 158 (2003) 27-36.
411 [55] H.Y. Chen, O. Zahraa, M. Bouchy, Inhibition of the adsorption and photocatalytic
412 degradation of an organic contaminant in an aqueous suspension of TiO_2 by inorganic ions, J.
413 Photochem. Photobiol. A 108 (1997) 37-44.
414 [56] L. Wenhua, L. Hong, C. Sao'an, Z. Jianqing, C. Chunan, Kinetics of photocatalytic
415 degradation of aniline in water over TiO_2 supported on porous nickel, J. Photochem. Photobiol.
416 A 131 (2000) 125-132.
417 [57] M. Abdullah, G.K. Low, R.W.E. Matthews, Effects of common inorganic anions on rates
418 of photocatalytic oxidation of organic carbon over illuminated titanium dioxide, J. Phys. Chem.
419 94 (1990) 6820-6825.